Figure S1

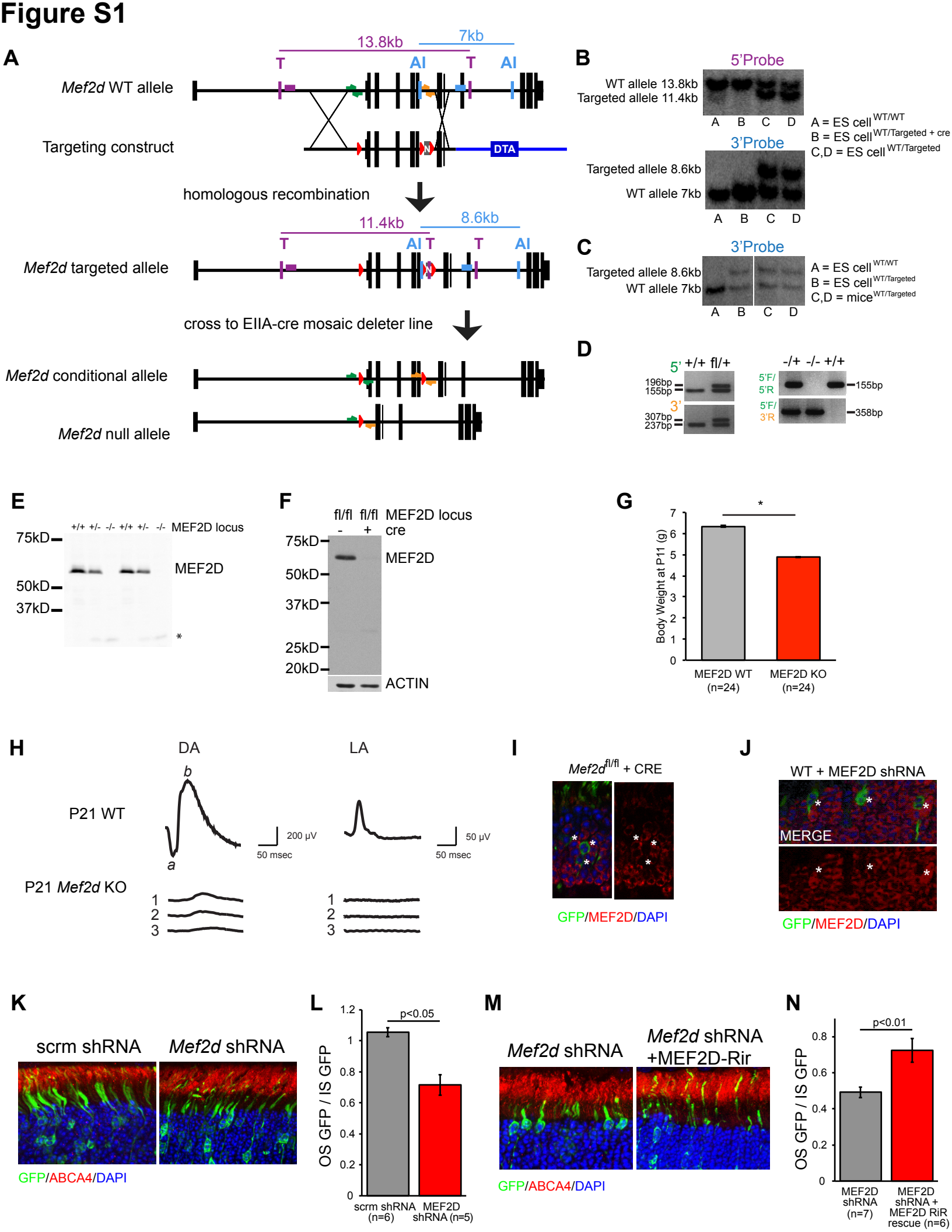
A
13.8kb
7kb
T
AI
T
AI
Mef2d WT allele
Targeting construct
DTA
homologous recombination
11.4kb
8.6kb
Mef2d targeted allele
cross to EIIA-cre mosaic deleter line
Mef2d conditional allele
Mef2d null allele
B
5'Probe
WT allele 13.8kb
Targeted allele 11.4kb
A B C D
A = ES cell WT/WT
B = ES cell WT/Targeted + cre
C,D = ES cell WT/Targeted
3'Probe
Targeted allele 8.6kb
WT allele 7kb
C
3'Probe
A = ES cell WT/WT
B = ES cell WT/Targeted
C,D = mice WT/Targeted
D
5' +/+ fl/+
196bp
155bp
3'
307bp
237bp
-/+ -/- +/+
5'F/
5'R
155bp
5'F/
3'R
358bp
E
+/+ +/- -/- +/+ +/- -/- MEF2D locus
75kD
MEF2D
50kD
37kD
*
F
fl/fl fl/fl MEF2D locus
- + cre
75kD
MEF2D
50kD
37kD
25kD
20kD
ACTIN
G
Body Weight at P11 (g)
MEF2D WT (n=24)
MEF2D KO (n=24)
H
DA
LA
P21 WT
b
a
200 µV
50 msec
50 µV
50 msec
P21 Mef2d KO
1
2
3
I
Mef2d fl/fl + CRE
GFP/MEF2D/DAPI
J
WT + MEF2D shRNA
MERGE
GFP/MEF2D/DAPI
K
scrm shRNA
Mef2d shRNA
GFP/ABCA4/DAPI
L
p<0.05
OS GFP / IS GFP
scrm shRNA (n=6)
MEF2D shRNA (n=5)
M
Mef2d shRNA
Mef2d shRNA +MEF2D-Rir
GFP/ABCA4/DAPI
N
p<0.01
OS GFP / IS GFP
MEF2D shRNA (n=7)
MEF2D shRNA + MEF2D RiR rescue (n=6)

Figure S2

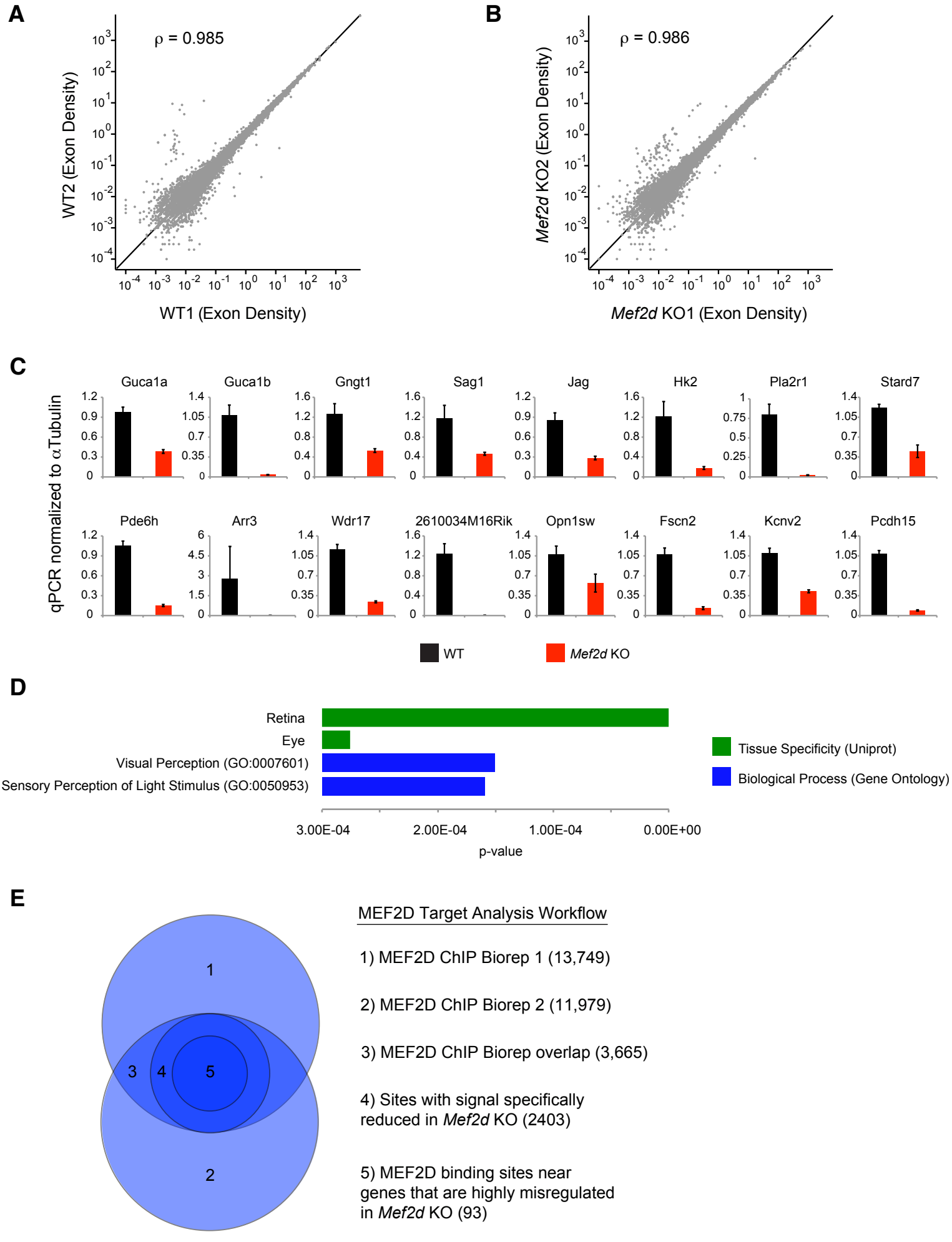
A
ρ = 0.985
WT2 (Exon Density)
WT1 (Exon Density)
B
ρ = 0.986
Mef2d KO2 (Exon Density)
Mef2d KO1 (Exon Density)
C
qPCR normalized to αTubulin
Guca1a
Guca1b
Gngt1
Sag1
Jag
Hk2
Pla2r1
Stard7
Pde6h
Arr3
Wdr17
2610034M16Rik
Opn1sw
Fscn2
Kcnv2
Pcdh15
WT
Mef2d KO
D
Retina
Eye
Visual Perception (GO:0007601)
Sensory Perception of Light Stimulus (GO:0050953)
Tissue Specificity (Uniprot)
Biological Process (Gene Ontology)
3.00E-04
2.00E-04
1.00E-04
0.00E+00
p-value
E
1
2
3
4
5
MEF2D Target Analysis Workflow
1) MEF2D ChIP Biorep 1 (13,749)
2) MEF2D ChIP Biorep 2 (11,979)
3) MEF2D ChIP Biorep overlap (3,665)
4) Sites with signal specifically reduced in Mef2d KO (2403)
5) MEF2D binding sites near genes that are highly misregulated in Mef2d KO (93)

Figure S3

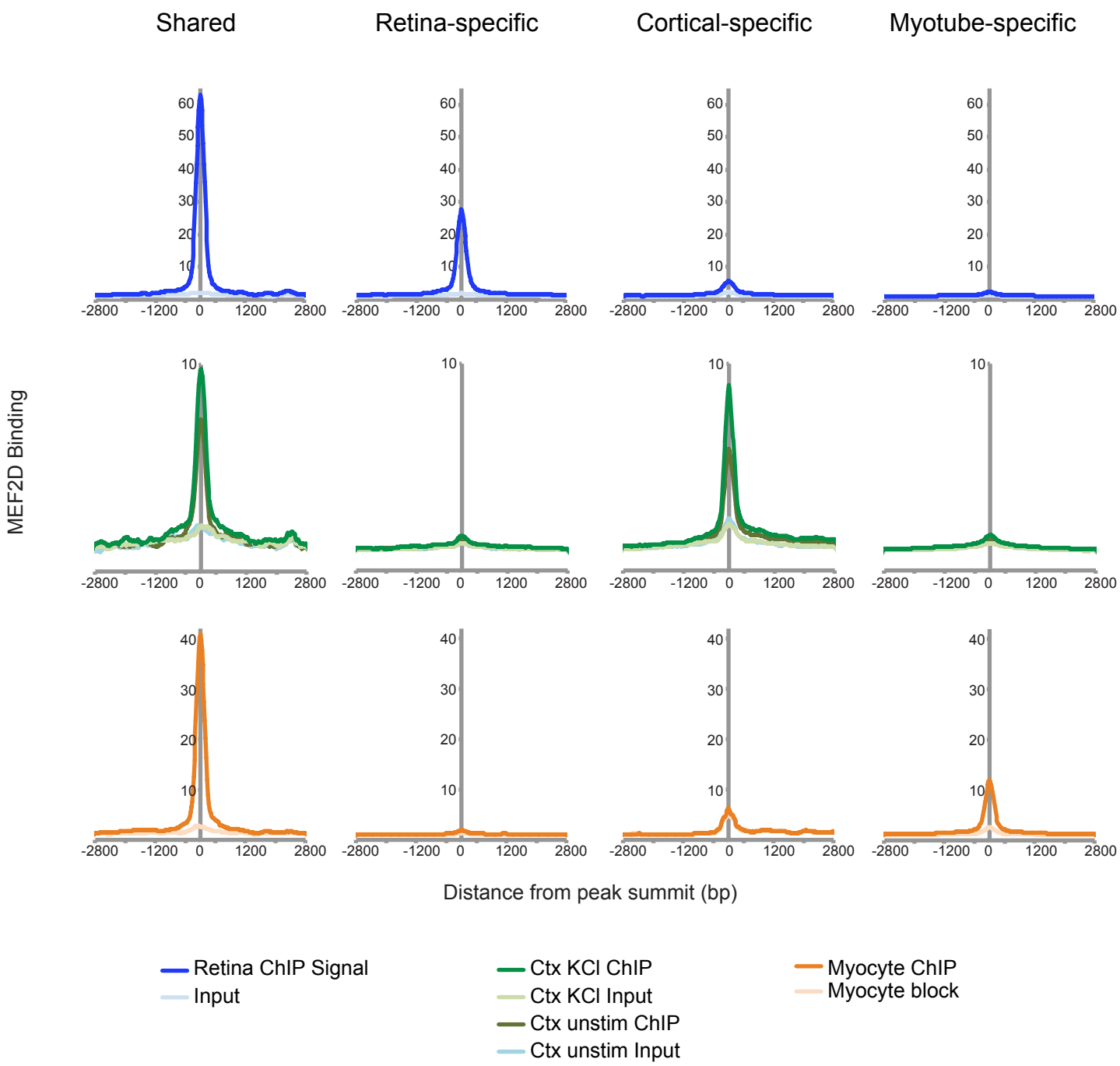
Shared
Retina-specific
Cortical-specific
Myotube-specific
MEF2D Binding
Distance from peak summit (bp)
Retina ChIP Signal
Input
Ctx KCl ChIP
Ctx KCl Input
Ctx unstim ChIP
Ctx unstim Input
Myocyte ChIP
Myocyte block

Figure S4

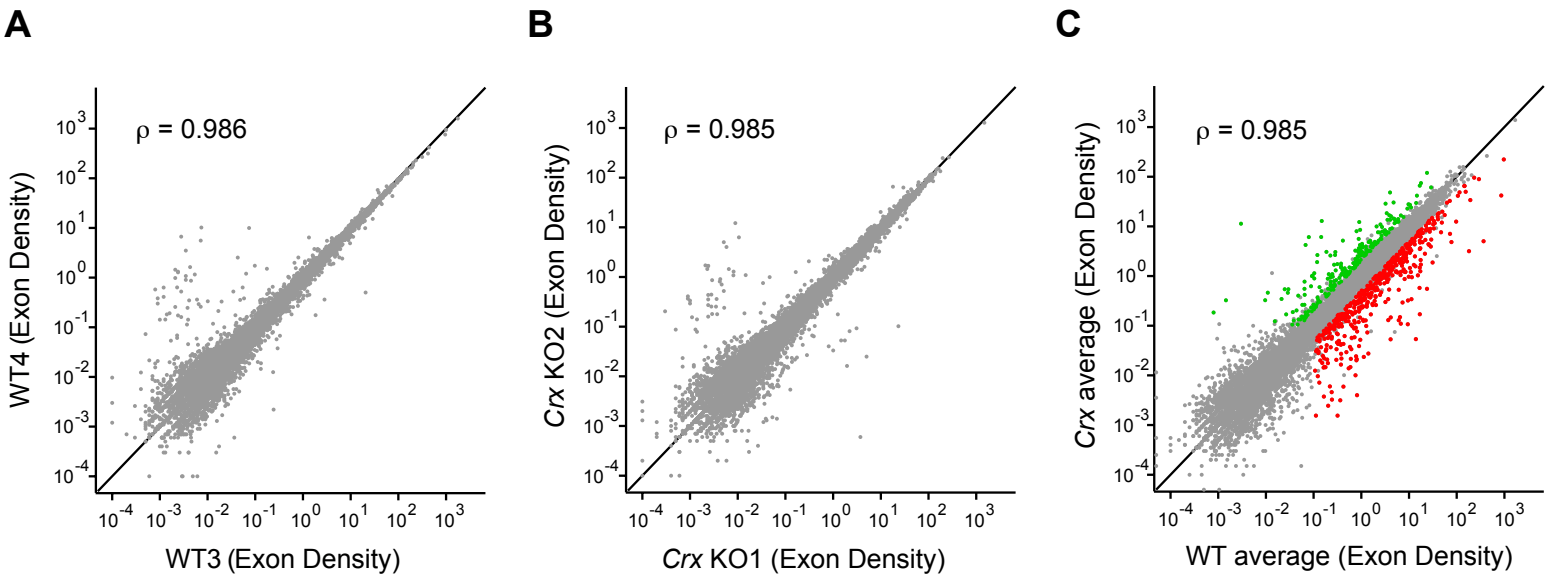
A
B
C
ρ = 0.986
ρ = 0.985
ρ = 0.985
WT4 (Exon Density)
WT3 (Exon Density)
Crx KO2 (Exon Density)
Crx KO1 (Exon Density)
Crx average (Exon Density)
WT average (Exon Density)

Figure S5

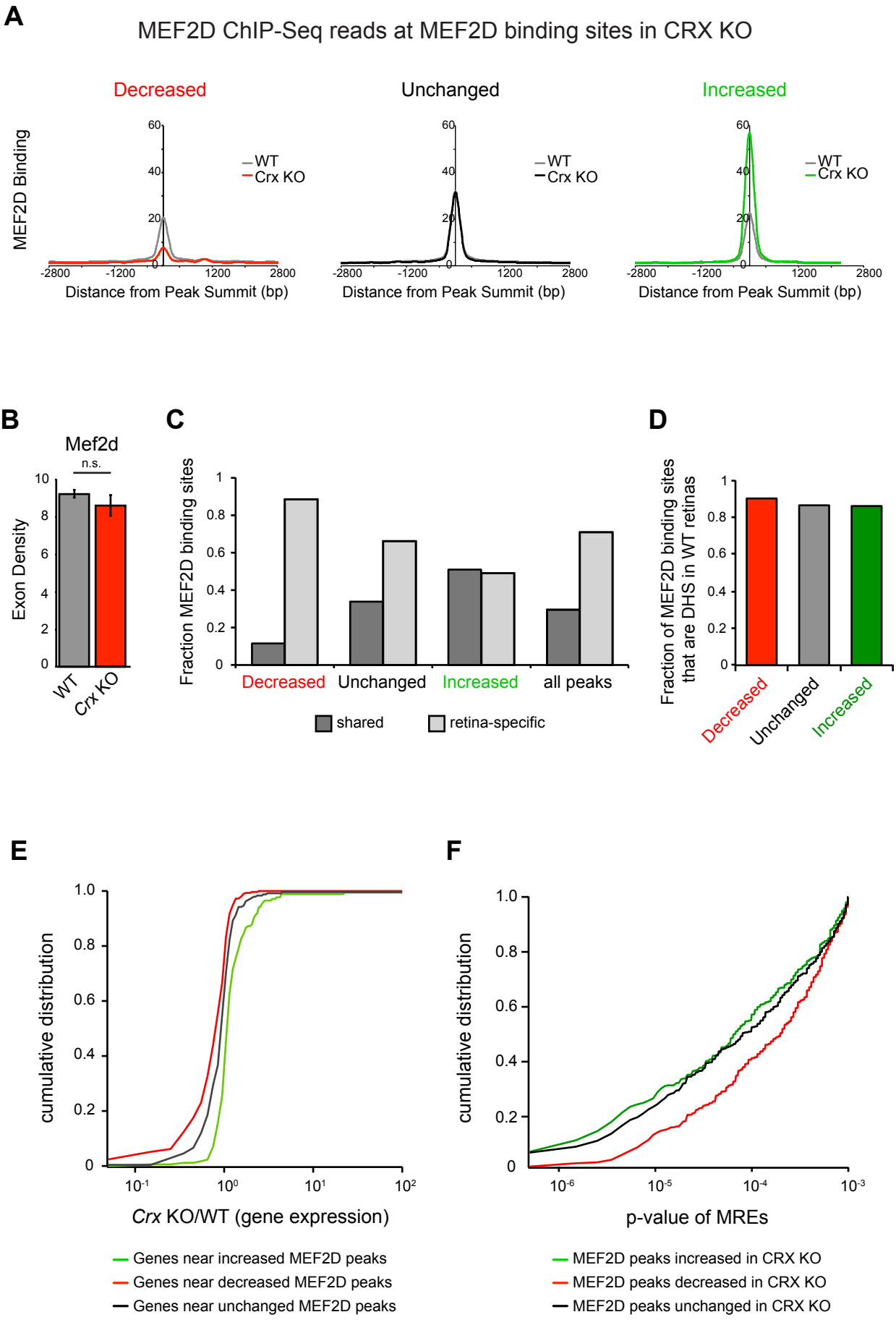
A
MEF2D ChIP-Seq reads at MEF2D binding sites in CRX KO
Decreased
Unchanged
Increased
MEF2D Binding
WT
Crx KO
Distance from Peak Summit (bp)
B
Mef2d
n.s.
Exon Density
C
Fraction MEF2D binding sites
Decreased
Unchanged
Increased
all peaks
shared
retina-specific
D
Fraction of MEF2D binding sites that are DHS in WT retinas
E
cumulative distribution
Crx KO/WT (gene expression)
Genes near increased MEF2D peaks
Genes near decreased MEF2D peaks
Genes near unchanged MEF2D peaks
F
p-value of MREs
MEF2D peaks increased in CRX KO
MEF2D peaks decreased in CRX KO
MEF2D peaks unchanged in CRX KO

Figure S6

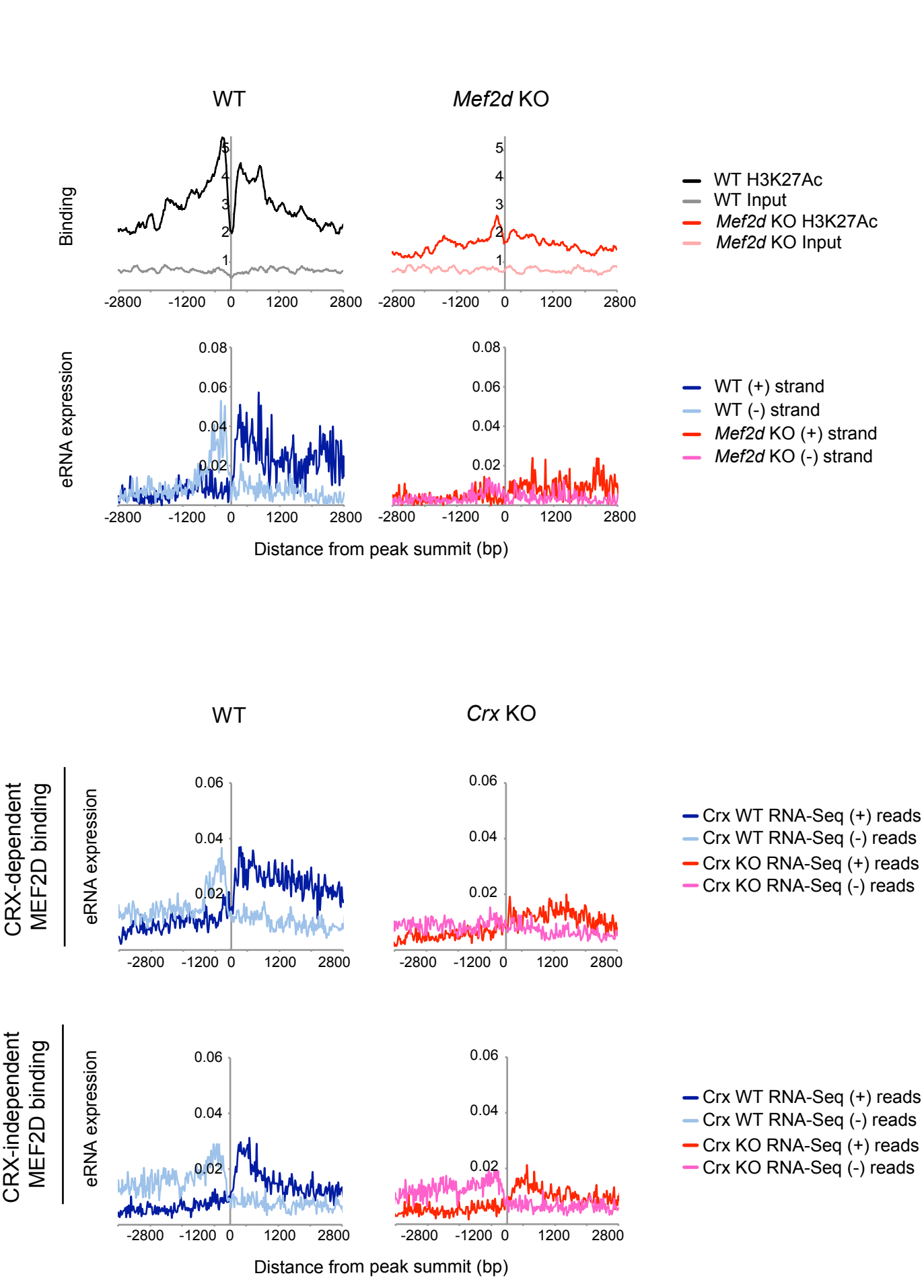
A
WT
Mef2d KO
Binding
eRNA expression
WT H3K27Ac
WT Input
Mef2d KO H3K27Ac
Mef2d KO Input
WT (+) strand
WT (-) strand
Mef2d KO (+) strand
Mef2d KO (-) strand
Distance from peak summit (bp)
B
WT
Crx KO
CRX-dependent MEF2D binding
CRX-independent MEF2D binding
eRNA expression
Crx WT RNA-Seq (+) reads
Crx WT RNA-Seq (-) reads
Crx KO RNA-Seq (+) reads
Crx KO RNA-Seq (-) reads
Distance from peak summit (bp)

Supplemental information

Supplemental Figure Legends

Figure S1. Generation and validation of a novel line of Mef2d KO mice and analysis of the *Mef2d* loss-of-function retinal phenotype. Figure S1 relates to Figure 1. (A) Schematic of the Mef2d gene targeting strategy. (Top) *Mef2d* WT allele aligned with the corresponding part of the targeting construct. The Mef2d allele was targeted by flanking exons 2 through 6 of the Mef2d genomic locus with loxP sequences (red triangles). Exons 2 and 3 include the highly conserved MEF2 and MADS domains critical for DNA-binding and MEF2 dimerization. A neomycin positive selection cassette (N) was inserted with a 3rd loxP site at the 3' end of the targeted region and Diphtheria toxin A (DTA) served as a negative selection marker. (Middle) Targeted ES cells were selected by resistance to G418 (and survival, and therefore lack of DTA) and analyzed by Southern analysis. Purple and light blue boxes represent relative positions external to the targeted region of 5' and 3' southern blot probes, respectively, and southern blot enzyme digestion sites are denoted in corresponding colors as T (Tth111I) and AI (ApaI) for 5' and 3' southern analysis of ES cells. Distances between endogenous Tth111I or ApaI restriction sites for southern blot analysis are illustrated in purple and light blue above the WT and targeted alleles. Successfully targeted ES cells were then injected into pseudopregnant females, and subsequent progeny were assessed for successful germline transmission of the targeted allele. (Bottom) Mice carrying the targeted allele were crossed to EIIA-cre germline deleter mice to generate Mef2d KO mice, where the entire region between the most 5' and 3' loxP sites was deleted, and *Mef2d*$^{fl/fl}$ conditional mice, where only the neomycin cassette was removed by Cre but two loxP sites remained in a now otherwise WT locus. Green and yellow arrows denote relative positions of PCR genotyping primers. (B) Southern blot analysis of WT and targeted *Mef2d* alleles in ES cells. Southern blot analysis of Tth111I (top) or ApaI (bottom)-

digested genomic DNA from targeted ES cells using 5' or 3' probes (purple and blue boxes in Figure S1A, respectively) indicates correct targeting of the Mef2d genomic locus. Expected genomic DNA fragment lengths are illustrated in Figure S1A above. (C) Southern analysis of mice with WT or targeted *Mef2d* alleles. Southern blot performed as described above using ApaI-digested genomic DNA from mouse liver and the same 3' probe described in Figure S1B. Genomic fragment lengths indicate that mice carry the correctly targeted Mef2d locus. (D) Polymerase chain reaction (PCR) results for routine genotyping of *Mef2d* knockout or conditional knockout mice. Genotyping for the conditional *Mef2d* floxed allele was performed by PCR using primer pairs 5'F (5′-gggttcagtccccagtgtaa-3′) and 5'R (5′- ccccctagtcagagcttgtg-3′) (Figure S1A, green arrows) as well as 3'F (5′-tgagggtaaccatgtgcttg-3′) and 3'R (5′-aaggcctggagagaaggtgt-3′), which span the 5' and 3' loxP sites introduced in introns I and VI, respectively (schematized in Figure S1A, yellow arrows). Genotyping for the constitutive *Mef2d* knockout was performed by PCR using primers as described above in the following pairs: 5'F and 5'R, or 5'F and 3'R, to test for the presence of a WT or null allele, respectively. 5'F and 3'R are sufficiently far away on the WT allele that a productive PCR reaction is only observed with a null allele. (E) Absence of full-length MEF2D protein in Mef2d KO mice. Western blot of MEF2D in whole brain lysates in Mef2d KO mice and littermates heterozygous or WT for Mef2d. An antibody that recognizes part of the protein C-terminal to the exons deleted in the Mef2d targeting strategy demonstrates complete loss of the full-length protein in the KO mice. A small, truncated product appears in Mef2d KO lysates with very low levels of expression (asterisk). (F) Effective removal of conditional Mef2d allele. Western blot of MEF2D in whole brain lysates of a Mef2dfl/fl mouse with nestin-cre and a littermate Mef2dfl/fl mouse with no Cre. Actin was used as a loading control. (G) Mef2d KO mice have reduced body weight. Mef2d KO mice were weighed at p11 along with a paired WT littermate. N=24 pairs. Graph displays mean +/- SEM. *p=1.35e-6. (H) Electroretinograms (ERGs) at P21 from a representative WT mouse and 3 MEF2D KO littermates under dark-adapted (DA) and light-adapted (LA) conditions. The MEF2D

KO mice all had subnormal dark-adapted (rod-dominant) responses and light-adapted (cone-isolated) responses that were indistinguishable from the lower limit of detectability (1μV). Comparing the mean dark-adapted and light-adapted $\log_e$ b-wave amplitudes of 3 WT mice with those of the 3 KO littermates revealed approximately 95% and ≥99% reductions, respectively, in the latter (Student's *t* test, p=0.0008 and p<0.0001). (I) Immunofluorescence of MEF2D (red) and GFP (green) from *Mef2d*$^{fl/fl}$ retinas electroporated at P0 with a construct expressing Cre-IRES-GFP and harvested at P21 (white asterisks designate electroporated cells). (J) Immunofluorescence of MEF2D (red) and GFP (green) from WT retinas electroporated at P0 with a construct expressing MEF2D shRNA and GFP and harvested at P21 (white asterisks designate electroporated cells). (K) Immunofluorescence of ABCA4 (red) to label photoreceptor outer segments (OS) and GFP (green) to label electroporated photoreceptors from WT retinas electroporated at P0 with a construct expressing either a scrambled control shRNA construct (scrm) or MEF2D shRNA and GFP and harvested at P21. (L) Mean GFP intensity in the ABCA4-positive region (OS GFP) was normalized to mean GFP intensity in the inner segments (IS GFP) to measure OS development while controlling for electroporation density (scrm shRNA, N=6; MEF2D shRNA, N=5 retinas). Error bars represent S.E.M. (M) Immunofluorescence of ABCA4 (red) to label photoreceptor outer segments and GFP (green) to label electroporated photoreceptors from WT retinas electroporated at P0 with a construct expressing either a MEF2D shRNA and GFP or MEF2D shRNA, and RNAi-resistant Mef2d rescue construct (MEF2D RiR) and GFP and harvested at P21. (N) Mean GFP intensity in the ABCA4-positive region (OS GFP) was normalized to mean GFP intensity in the inner segments (IS GFP) to measure OS development while controlling for electroporation density (scrm shRNA, N=7; MEF2D shRNA, N=6 retinas). Error bars represent S.E.M.

Figure S2. Identification and characterization of direct MEF2D target genes in p11 retinas. Figure S2 relates to Figure 2. (A) RNA-seq average exon densities for individual genes in two

P11 WT retinal samples are displayed in gray (ρ=Spearman rank correlation coefficient). Each sample was prepared from the two, pooled retinas of an individual mouse. Samples were collected from one male WT mouse (WT1; x-axis) and one female WT mouse (WT2; y-axis) to identify MEF2D targets that are shared in both male and female retinas in subsequent analyses. Expected sexual differences in retinal gene expression were observed. (B) RNA-seq average exon density for individual genes in two P11 retinal samples as described in (A), but from one male *Mef2d* KO mouse (x-axis) and one female *Mef2d* KO mouse (y-axis) (ρ=Spearman rank correlation coefficient). (C) qPCR validation of RNA-seq results for selected MEF2D target genes; n=3 for each data point. Error bars represent S.E.M. Student's *t* test, $p<0.05$ for all genes with the exception of Arr3 p=0.13. (D) DAVID analysis of tissue-specificity and functional enrichment for 185 highly misregulated genes in Mef2d KO retinas compared to WT retinas. (E) Schematic analysis workflow for identifying MEF2D-bound sites necessary for retinal gene expression.

Figure S3. Shared and tissue-specific binding of MEF2D. Figure S3 relates to Figure 3. Aggregate plots of MEF2D binding to shared or tissue-specific enhancers in P11 retinas, cultured cortical neurons before and after membrane depolarization and cultured myocytes (myocyte data from Sebastian et al., 2013) as determined by average read density. Aggregate plots were normalized to total peak numbers in each tissue.

Figure S4. Gene expression in WT versus *Crx* KO retinas at P11. Figure S4 relates to Figure 4. A) RNA-seq exon densities for individual genes in two P11 WT retinal samples are displayed in gray. Each sample was prepared from the two, pooled retinas of an individual mouse. Samples were collected from one male WT mouse (x-axis) and one female WT mouse (y-axis) to identify CRX target genes that are shared in both male and female retinas in

subsequent analyses. Expected sexual differences in retinal gene expression were observed. (B) RNA-seq exon densities for individual genes in two P11 retinal samples, as described in (A), but from one male *Crx* KO mouse (*Crx* KO1; x-axis) and one female *Crx* KO mouse (*Crx* KO2; y-axis). (C) RNA-seq average exon density for individual genes in P11 WT and *Crx* KO retinas are displayed in gray (n=2 per genotype). Genes were considered upregulated (green) or downregulated (red) only if expressed at >0.1 in 2 WT or 2 KO samples, if KO/WT exon density was ≥2x or <0.5 and if the p-value of the KO versus WT log-data pairs was <0.05 (Student's *t* test).. ρ=Spearman rank correlation coefficient.

Figure S5. Characterization of MEF2D-binding in WT and *Crx* KO retinas. Figure S5 relates to Figure 5. (A) Aggregate plots of MEF2D binding at sites where MEF2D binding is decreased, unchanged or increased in *Crx* KO retinas compared to WT retinas, as determined by ChIP-seq average read density. (B) Mef2d transcript expression (exon density) in WT and *Crx* KO P11 retinas (n.s., not significant). (C) Distribution of shared versus retina-specific MEF2D binding sites among sites where MEF2D binding is decreased, unchanged or increased in P11 *Crx* KO retinas compared to WT retinas. (D) Fraction of sites where MEF2D binding is increased (green), unchanged (gray) or decreased (red) in *Crx* KO retinas that overlap DNase I hypersensitive sites (DHS) in WT retinas. (E) Distribution of gene expression ratios (*Crx* KO/WT) in P11 retinas for genes proximal to MEF2D binding sites where MEF2D binding is decreased, unchanged or increased in P11 *Crx* KO retinas compared to WT retinas as determined by RNA-seq exon density. Genes near sites where MEF2D binding decreases in *Crx* KO retinas have significantly lower *Crx* KO/WT ratios of expression compared to genes near sites where MEF2D-binding is unchanged (KS test; p=2.57e-5). Genes near sites where MEF2D binding increases in *Crx* KO retinas have significantly higher *Crx* KO/WT ratios of expression compared to genes near sites where MEF2D-binding is unchanged (K-S test; p=5.92e-9). (F) Strength of MEF2 responsive element consensus sequences (MREs) at MEF2D

binding sites where MEF2D binding is decreased, unchanged or increased in P11 *Crx* KO retinas compared to WT retinas. The strengths of MREs at sites where MEF2D binding decreases in *Crx* KO retinas are significantly lower than MREs at sites where MEF2D binding increases (K-S test; 4.76e-5) or where MEF2D binding is unchanged (K-S test; p=2.16e-4).

Figure S6. H3K27Ac levels and eRNA expression at MEF2D-bound enhancers in WT, *Mef2d* KO and *Crx* KO retinas. Figure S6 relates to Figure 6. (A) (Top) Aggregate plot of H3K27ac levels at MEF2D target gene enhancers in P11 WT versus *Mef2d* KO retinas (Student's *t* test; p=7.16e-18). (Bottom) Aggregate plot of eRNA expression at MEF2D target gene enhancers in P11 WT versus *Mef2d* KO retinas (t-test; p=1.12e-7). (B) (Top) Aggregate plots of eRNA expression at MEF2D-bound enhancers that require CRX for MEF2D binding in P11 WT versus *Mef2d* KO retinas. (Bottom) Aggregate plots of eRNA expression at MEF2D-bound enhancers that do not require CRX for MEF2D binding in P11 WT versus *Mef2d* KO retinas.

EXTENDED EXPERIMENTAL PROCEDURES

Immunoblotting

Dissected retinas were homogenized in RIPA buffer (50 mM Tris pH 8.0, 150 mM NaCl, 1% Triton-X-100, 0.5% sodium deoxycholate, 0.1% SDS, 5 mM EDTA, 10 mM NaF, 1 mM sodium orthovanadate, complete protease inhibitor cocktail tablet (Roche)) and protein levels were measured using the Bradford method (BioRad). 15µg of each protein sample was used. Conventional western blotting used enhanced chemiluminescence and HRP-conjugated secondary antibodies. Commercial antibodies used include anti-MEF2D (mouse 1:1000, BD Biosciences), anti-MEF2C (rabbit 1:1000, Abcam ab64644) and anti-GAPDH (rabbit 1:5000, Sigma). An anti-MEF2A antibody was raised in rabbit against amino acids 272-484 of human

MEF2A (1:1000).

Immunofluorescence

For immunostaining experiments retinas or eyecups were fixed in 4% formaldehyde in phosphate buffered saline (PBS), equilibrated in sucrose and then frozen in a 1:1 solution of 30% sucrose in 1x PBS Tissue-Tek O.C.T. (Sakura). 20μm cryo-sections were generated on a Leica CM1950 cryostat and mounted on slides. Sections were incubated in block solution (10% goat serum and 0.25% Triton X-100 in 1XPBS) for 1 hour and then incubated with primary antibodies in block solution for 2 hours at room temperature or 4° C overnight. Alexa dye-conjugated secondary antibodies were used at 1:500 dilutions in block solution (Life Technologies). Primary antibodies were anti-MEF2D (mouse 1:1000, BD Biosciences 610775), anti-MEF2A (rabbit 1:1000, generated in the Greenberg lab) and anti-GFP (chicken 1:1000, Aves Labs GFP-1020). Slides were mounted using Prolong Gold AntiFade reagent with 4′,6-diamidino-2-phenylindole (DAPI) (Life Technologies). Images were acquired on a Olympus FV1000 confocal microscope at 1024x1024 pixel resolution or using a Zeiss Axio Imager microscope with a 63x objective with the use of an apotome.

Generation of MEF2D knockout mice and in vivo phenotype analysis

The targeting construct used for homologous recombination in ES cells was cloned using nested PCR amplification from mouse sv129 genomic DNA into a vector containing a floxed neomycin-resistance positive selection cassette (NEO) and a diphtheria toxin A negative-selection cassette (DTA) (Figure S1A). The final targeting construct inserted one loxP site into intron I and two loxP sites flanking a NEO cassette into intron VI. Care was taken to place loxP sites and the NEO cassette in non-conserved regions of the intron. The region between loxP sites flanked a 5.1kb region of the *Mef2d* locus that spanned exons 2-6. This included the first five coding exons of MEF2D including the translational start site and the conserved MADS and

MEF2 domains, which include the critical DNA and protein binding residues of MEF2D. The arms used flanking the targeted region were 4.1kb 5' and 2kb 3' to the targeted regions.

All targeting constructs were confirmed by direct sequencing in their entirety prior to use in gene targeting. The constructs were linearized and electroporated into J1 ES cells. Genomic DNA isolated from G418-resistant ES cell clones was screened by Southern blot. 5' and 3' probes external to the genomic fragment contained within the targeting vector were used. For the 5' southern, ES cell DNA was digested with Tth111I and positive targeting was indicated by a 2.4 kb decrease in the digested fragment due to a new Tth111I digest site in the NEO cassette (Figure S1B). The 3' side was analyzed by digesting ES cell DNA with ApaI and positive targeting was indicated by a 1.6 kb increase in the size of the digested product as compared to wild-type ES cell genomic DNA representing the presence of the NEO cassette in the *Mef2d* endogenous locus (Figure S1B). ES cell clones positive for correct targeting of the *Mef2d* locus by Southern screening were karyotyped and those with confirmed normal karyotypes were used to generate mice.

Two confirmed MEF2D targeted ES cell clones were injected into C57BL/6 blastocysts and subsequently implanted into pseudopregnant females. The resulting chimeric offspring were mated with C57BL/6 mice, and the agouti offspring were screened by PCR genotyping to confirm germline transmission of the mutant allele. Targeted mice were then crossed to EIIA-CRE expressing mice (stock number 003724; The Jackson Laboratory) and offspring were analyzed for expression of the Cre allele and the state of the targeted MEF2D allele using PCR genotyping. Mice that expressed Cre and had excised either the neomycin cassette or the full targeted region were bred to wildtype C57BL/6 mice and offspring that no longer expressed Cre and had transmission of either the floxed allele or the null allele without neomycin were used to establish mouse lines.

Mice were analyzed for gross phenotypes by preservation in Bouin's Solution (Sigma) and histology using hematoxylin and eosin staining of tissues throughout the mouse. Results were reviewed with a pathologist.

Animal husbandry and colony management

For routine experimentation, animals were genotyped using a PCR-based strategy. CRX knockout mice were obtained from The Jackson Laboratories (stock number 007064) and genotyped according to their protocols. Animals harboring the *Mef2d* null allele were genotyped with a forward primer upstream of *Mef2d* exon 2 and a reverse primer either 155bp downstream (for the WT allele) or a reverse primer just downstream of exon 6 (for the null allele).

Conditional knockout animals were genotyped for the presence of the loxP site, which shifts the size of the PCR product. See Figure S1 for PCR product sizes and primer sequences. All experiments described here were performed using animals derived from a sv129/C57BL/6 hybrid genetic background, with the mutation backcrossed in the C57BL/6 background (Charles River Laboratories) between 3 and 8 generations.

Semi-Thin microscopy

Retinas were dissected and eyecups were fixed with 2% formaldehyde and 2.5% glutaraldehyde in 0.15 M Sorenson's phosphate buffer (pH 7.4), followed by 1% OsO4, 1.5% potassium ferrocyanide, and stained en bloc with 1% uranyl acetate. 0.5-1 μM thick sections of the eyecup were stained with toluidine blue and examined with a Nikon Eclipse E600 microscope.

Electroretinograms

Mice were dark-adapted overnight and anesthetized with sodium pentobarbital injected intraperitoneally prior to testing. Pupils of each animal were topically dilated with phenylephrine hydrochloride and cyclopentolate hydrochloride, and mice were then placed on a heated platform. Rod dominated responses were elicited in the dark with 10-μs flashes of white light (1.37 x 105 cd/m^2) presented at intervals of 1 minute in a Ganzfeld dome. Light-adapted, cone responses were elicited in the presence of a 41 cd/m^2 rod-desensitizing white background with the same flashes (1.37 x 105 cd/m^2) presented at intervals of 1 Hz. ERGs were monitored with a silver wire loop electrode in contact with the cornea topically anesthetized with proparacaine hydrochloride and wetted with Goniosol and with a cotton wick electrode in the mouth as the reference; an electrically-shielded chamber served as ground.

All responses were differentially amplified at a gain of 1,000 (-3db at 2 Hz and 300 Hz; AM502, Tektronix Instruments, Beaverton, OR), digitized at 16-bit resolution with an adjustable peak-to-peak input amplitude (PCI-6251, National Instruments, Austin, TX), and displayed on a personal computer using custom software (Labview, version 8.2, National Instruments). Independently for each eye, cone responses were conditioned by a 60 Hz notch filter and an adjustable artifact-reject window, summed (n=4-20), and then fitted to a cubic spline function with variable stiffness to improve signal:noise without affecting their temporal characteristics; in this way we could resolve cone b-wave responses as small as 1 μV.

Quantification of outer segment disruption

Immunohistochemistry was performed as described above. Primary antibodies used were anti-ABCA4 (mouse, 1:1000, Novus Biologicals NBP1-30032) and anti-GFP. For quantification, images were acquired using a Zeiss Axio Imager microscope with a 63x objective with the use of an apotome. Microscope settings were optimized for each image with settings selected such that no pixels were beyond the range of the detector. For each neuron, a Z-stack of 10 sections

with a step size of 1μm was collected, and a maximal intensity projection was created and used for analysis. Retinas were analyzed blind to genotype or experimental condition. ImageJ was used for processing. Initial defining of areas for analysis was done blind to GFP-image, using ABCA4 and DAPI layers only. Regions of interest (ROI) were obtained for both outer segments (OS, ABCA4-positive) or inner segments as the control for electroporation efficiency and signal intensity (IS, between ABCA4+ and DAPI+ areas). Mean pixel intensity was quantified for GFP in the OS and IS ROI and an index of photoreceptor apical process growth was defined as mean GFP in OS/ mean GFP in IS. Mean values for an experimental condition were determined from at least 3 retinas imaged from at least 2 different sections. Mean index data from each retina was used to analyze significance by Student's t-test.

Plasmids

Previously characterized MEF2D shRNA and mutant shRNAs cloned into the pLL3.7 vector (Addgene Plasmid 11795) were used (Flavell et al., 2006; Lin et al., 2008). Mouse MEF2D cDNA was made resistant to MEF2D-specific shRNA by mutating the sequence 5'-AGCTCTCTGGTC-3'; to 5'-AGCTC**A**CT**A**GTC-3' (mutations in bold) using site-directed mutagenesis (Agilent Technologies). The cDNA was then cloned into the pFUIGW vector (Zhou et al., 2006).

In vivo retinal electroporations

Adapted from (Cherry et al., 2011; Matsuda and Cepko, 2008) with the following modifications: approximately 0.75μl DNA for electroporation were injected into the subretinal space of p0 mice using a Nanoject II and pulled glass needles (Drummond Scientific, Broomall, PA).

RNA isolation, reverse transcription & qPCR

Total RNA was extracted with Trizol reagent (Life Technologies) followed by column purification

using the RNeasy Micro kit (Qiagen) with on-column DNAse digestion. RNA quality was assessed on a 2100 Bioanalyzer (Agilent). RNA was reverse transcribed with the High Capacity cDNA Reverse Transcription kit (Life Technologies). Real-time quantitative PCR analysis was carried out using the StepOnePlus qPCR system and Power SYBR Green mix (Life Technologies). Reactions were run in duplicates or triplicates and *Tuba1* levels were used as an endogenous control for normalization. Real-time PCR primers were selected from an existing database (Origene). Primer sequences available upon request.

RNA-Seq sequencing and analysis

RNA-Seq was performed to a depth of at least $8x10^7$ clean reads per sample. Two biological replicates were performed for each genotype and used in the analyses described below. Mapping of RNA-Seq reads and subsequent analysis of read-densities across all UCSC annotated genes was performed as described (Kim et al., 2010). Exon read density was calculated based on number of read bases per exon length, with total number per sample renormalized to 10 million 35-bp reads.

Misregulated genes were defined using the following criteria: To be considered, genes needed to be expressed at a read density level of >0.1 in either both WT datasets, or both KO datasets. Genes were considered misregulated if KO/WT was >2 or <0.5, and the log p-value of the KO versus WT datasets was <0.05 (paired t-test).

To evaluate which biological processes might be enriched in our misregulated genes, we used the DAVID Functional Annotation web tool (http://david.abcc.ncifcrf.gov), limiting our analysis to DAVID's GO biological process FAT category. DAVID was also used to determine tissue enrichment of the gene sets (Dennis et al., 2003; Huang da et al., 2009a, b).

Chromatin Immunoprecipitation

P11 mouse retinas were dissected in ice-cold HBSS prior to homogenization and crosslinking. 4µg of anti-MEF2D antibody was pre-bound to 15µl of Protein A dynabeads (Life Technologies) per immunoprecipitation (IP) from approximately 100 million retinal cells. H3K27Ac ChIP was performed as described above with the following modifications: 10 mM sodium butyrate was added to all solutions until post-IP washes with the exception of cross-linking buffer. Chromatin was fragmented for H3K27Ac ChIP by brief sonication followed by MNase (New England Biolabs) digestion for 8 minutes at 37C to generate mononucleosomes. 0.25µg of anti-H3K27Ac antibody was used per IP from 10 million retinal cells. After reverse crosslinking all samples were purified using phenol/chloroform/isoamyl alcohol followed by column clean up (Qiagen, QIAquick PCR Purification Kit).

ChIP-qPCR

Quantitative PCR analysis of ChIP samples was carried out using the StepOnePlus qPCR system and Power SYBR Green mix (Life Technologies). Fraction of input values were calculated by comparing the average threshold cycle of the ChIP DNA to a standard curve generated using serial dilutions of input DNA. Fold enrichment for each genomic region evaluated was calculated as its fraction of input divided by the average fraction of input value calculated for standard background regions at least 2 kb away. Amplicon primers were designed using Primer3Plus (Untergasser et al., 2007). Primer sequences available upon request.

ChIP-Seq Sequencing, Data Processing and Peak Characterization

Two WT and one *Mef2d* KO anti-MEF2D ChIP samples were submitted to BGI (Shenzhen, China) for 50 base pair single end sequencing on the Illumina Hiseq 2000 platform. For each sample, over 20 million clean reads were obtained. Sequencing data was obtained from BGI in gzipped fastq file format. Sequencing reads were then aligned to the July 2007 assembly of the

mouse genome (NCBI 37, mm9) using the Burrows- Wheeler Aligner (BWA) with settings -q 0 -t 4 -n 5 -k 2 -l 32 -e -1 -o 0. The resulting bwa files were then converted to sam files and uniquely mapped reads were extracted from the sam files. Sam files of the uniquely mapped reads were then converted to bam files and bed files. SAMTools and BEDTools-2.16.2 were used for the above conversions. Chromosome names were changed using a custom perl script. Bed files were then used for peak calling using Model-based Analysis of ChIP-Seq (MACS) 1.4.0 (Zhang et al., 2008) with the following parameters: default parameters (p=1e-5) except -bw 200, and for histone marks, default parameters (p=1e-5) except --nomodel --shiftsize 73. Input was used as background for peak calling. To visualize ChIP-Seq data on the UCSC genome browser, reads in ChIP-Seq bed files were extended to 200 bp for transcription factors or 146 bp for histone marks using a custom perl script. BEDTools was then used to convert this file to bedgraph, at which point each file was normalized to 10 million total reads, then converted to bigwig track format and displayed as the number of input normalized ChIP-Seq reads.

MEF2D peaks were considered high confidence peaks if they appeared in 2 WT bioreplicates and the MEF2D ChIP-Seq read density in the WT peak was >=2.5X the read density in a MEF2D KO ChIP-Seq. Specifically, bioreplicate 1 had 13,749 peaks called by MACS over input chromatin. Bioreplicate 2 had 11,979 peaks. 3,665 peaks appeared in both replicates, and 2,403 of these peaks were down >=2.5x in the MEF2D KO as compared to its wildtype littermates (bioreplicate 2). We used this set of reproducible and specific MEF2D peaks for subsequent analysis. MEF2D peaks were classified based on their location relative to genes in the NCBI Reference Sequence Database (RefSeq). MEF2D peaks were classified as being proximal if they were within 1kb of an annotated transcriptional start site (TSS). MEF2D peaks were classified as being distal if they were greater than 1kb from an annotated transcriptional start site (TSS). Distal MEF2D peaks were further classified as intragenic if they occurred within a RefSeq gene (but not within 1kb of the TSS), or as extragenic if they did not occurred within a

RefSeq gene (and were greater than 1kb away from a TSS). For chromatin modifications (i.e. H3K27ac), the number of input-normalized ChIP-Seq reads within a two kb window centered on each binding site was taken to be the ChIP-Seq signal at the binding site. For transcription factors (e.g. MEF2D), the number of input-normalized ChIP-Seq reads within a 400 bp window centered on each binding site was taken to be the ChIP-Seq signal at the binding site. The number of reads was calculated using HOMER (annotatepeaks.pl; (Heinz et al., 2010)) except in the case of the initial MEF2D peak ChIP-Seq analysis between MEF2D WT and KO, where read density was calculated using a custom perl script for comparison.

For H3K27Ac ChIP, one bioreplicate of MEF2D WT versus KO retinas was sequenced together with their input samples. The number of input-normalized ChIP-Seq reads within a 2000 bp window centered on each binding site was taken to be the ChIP-Seq signal at the binding site.

Raw read data and accompanying bigWig files have been deposited with the Gene Expression Omnibus (GSE61392).

Cortical neuron cell culture and potassium chloride-mediated depolarization of cultured neurons

To obtain cortical neurons, mouse cortices were dissected from E16.5 C57BL/6 mouse embryos in dissection medium (DM) (10mM MgCL2, 10mM HEPES, 1mM kynurenic acid in 1X Hank's Balanced Salt Solution, pH 7.2) and then dissociated for 10 minutes in DM containing 20U/ml papain (Worthington Biochemicals) and 0.32 mg/ml L-cysteine (Sigma). Enzymatic dissociation was terminated by washing dissociated cells three times for two minutes each in DM containing 1% ovomucoid (Worthington Biochemicals) and 1% bovine serum albumin (Life Technologies). Cells were then triturated using a glass Pasteur pipette to fully dissociate cells. After dissociation, neurons were kept on ice until plating. Dissociated neurons were plated and

maintained in Neurobasal medium with B27 supplement (Life Technologies), 1 mM L- glutamine, and 100 U/mL penicillin/streptomycin for 7 days. For ChIP-Seq experiments, neurons were plated at an approximate density of 4x10^7 in 15 cm culture dishes pre-coated with a solution of 20 µg/ml poly-D-lysine (Sigma) and 4 µg/ml mouse laminin (Life Technologies) in water. Neuronal cultures were pre-treated with 1µM tetrodotoxin (TTX, Fisher) and 100µM DL-2-amino-5-phosphopentanoic acid (D-APV, Tocris Bioscience) overnight to reduce endogenous neuronal activity ("silencing") prior to stimulation. Neurons were membrane depolarized with 55 mM extracellular KCl by addition of prewarmed depolarization buffer (170 mM KCl, 2 mM CaCl2, 1 mM MgCl2, 10 mM HEPES pH7.5) to a final concentration of 31% in the neuronal culture medium in the plate. Neurons collected for ChIP were either only silenced or silenced with 2 hours of membrane depolarization.

Two bioreplicates were submitted for ChIP-sequencing. Each bioreplicate consisted of anti-MEF2D ChIP for both silenced and membrane depolarized samples, along with input controls. To maximize signal and specificity, ChIP-seq reads from membrane depolarized samples from both bioreplicates were combined and used to call peaks over combined input reads using MACS as described above. This was repeated to call peaks on the combined reads of 2 bioreplicates of silenced samples. To generate the most comprehensive peak list, silenced and membrane depolarized called MEF2D peaks were combined.

Previously published ChIP-Seq data sets

For comparison to retinal and cortical MEF2D ChIP-Seq datasets, we used previously published data for MEF2D isoform α1 and MEF2Dα1-blocked control ChIP-seq in myocytes (GSE43223) (Sebastian et al., 2013). In addition, we used ChIP-Seq data for two bioreplicates of CRX as well as an IgG control (GSE20012) (Corbo et al., 2010). Sequencing data for both datasets was mapped and peaks were called as described above using their respective controls as described.

CRX peaks used in analyses were those that appeared in both bioreplicates. Myocyte MEF2D peaks were called based on one bioreplicate.

ChIP-Seq analysis (peak overlap, data plots and motif enrichment)

For determining overlap of called peaks, intersectbed from BEDTools-2.16.2 was used with default settings except the –u option was used to get a list of each unique original feature that overlapped from one of the two compared groups instead of overlap regions or other outputs. 1 bp was sufficient to determine overlap.

HOMER 4.1 (Heinz et al., 2010) was used for the majority of the analysis of ChIP-Seq data. The mm9 genome was used for mapping and fasta file generation. ChIP tag directories were created using bed files of unextended reads and Homer MakeTagdirectory with fragment length specified as 200bp for sonicated samples (transcription factors) or 146bp for MNase digested samples (histone marks in retina).

For further analysis the following commands were used with the generated tag directories. Settings used were default unless specified otherwise. Counts of reads, or "Tag counts" were generated using annotatePeaks.pl with default options and a size of 400 bp centered on the peak summit for DHS and transcription factors, or a size of 2000 bp centered on the peak summit for histone marks. Genome-wide DNase I hypersensitivity (DHS) data from retinas of 8 week old mice was obtained from the ENCODE consortium, for which there was one bioreplicate used.

Aggregate plots were generated using annotatePeaks.pl with options –d -size 6000 -hist 20 for ChIP-seq data. Options for motif aggregate plots were –m -hist 20 -size 400.

De novo and known motif enrichment was performed using findMotifsGenome.pl with options -len 6,8,10,12 -S 15 –h. Regions used for motif calculations were 200bp around the peak summit. Unless otherwise specified, background for motif enrichment for each peak was an equally sized genomic window at the edge of the peak, provided the background region did not overlap with another peak in the relevant dataset. PWMs from top *de novo* motifs found were then put into TOMTOM from the MEME suite (Bailey et al., 2009) and evaluated for their similarity to motifs in the JASPAR Vertebrates and UniPROBE Mouse databases using a Pearson's correlation coefficient.

For a finer analysis of motif strength based on its similarity to a given PWM, FIMO from the MEME suite was used to identify motifs and their p-values based on provided PWMs and a p-value >=1e-4. Sequence FASTA files for input into FIMO were generated using Homer 4.1 homertools extract –fa. 200bp regions centered on the peak summit were used.

MEF2D-bound enhancers were classified into different categories based on the behavior of the eRNA read density (quantification described below) and quantified H3K27ac signal at each enhancer. Enhancers were classified as having H3K27ac if they had >10 normalized reads (tag count, per Homer) in a 2 kb window centered on the MEF2D peak summit. Enhancers with H3K27ac were classified as having a MEF2D-dependent decrease in H3K27ac if they exhibited a two fold or greater decrease in H3K27ac signal in MEF2D KO retinas.

Analysis of MEF2D peak size changes in *Crx* KO retinas

ChIP was performed using the anti-MEF2D antibody described above and one bioreplicate of Crx WT versus KO retinas was sequenced, each with its respective input as a control. Read

counts were determined in both samples again using a 400 bp window as described above. To identify changes in MEF2D binding in the Crx KO with high confidence, we compared the MEF2D read density in the Crx KO to three WT samples: the two bioreplicates originally used to identify MEF2D peaks, as well as the Crx WT littermate sample. Changing peaks were identified as those where the read density in the Crx KO was either 2x smaller or 2x larger than the average read density across the three WT samples. In addition, $p<0.0616$ was required using an unpaired one sided t-test.

Enhancer RNA (eRNA) Analysis

To define eRNAs, a 2kb window centered on the summit of each enhancer was defined. For extragenic enhancers, only those enhancers with a summit >2kb away from the end or TSS of a gene were considered. For intragenic enhancers, only those enhancers with a summit >1.2kb downstream of the TSS and >2kb away from the end of the gene or TSS of another gene were considered. Additionally, for intragenic enhancers the sense strand and its RNA-seq reads was removed from consideration. In order to be considered eRNAs, 3 reads were required within the 2kb window between the 2 WT samples combined. In addition, a z score of >= 1.645 was required for read number downstream of the peak summit versus upstream. This excluded enhancers with reads that were not sufficiently asymmetric on a given strand with respect to the enhancer summit, as eRNAs have been characterized as being located primarily downstream of enhancer peaks on each strand. For extragenic enhancers, a z score of >=1.645, indicating bias of RNA- seq reads downstream of the enhancer summit, was required on both strands. For intragenic enhancers, a z score of >=1.645 was required on only the anti-sense strand and sense reads were ignored. For enhancers that met these criteria, eRNA read density was then calculated in the 1kb region downstream of the enhancer summit only, which represented two 1kb windows for extragenic enhancers and one 1kb window for intragenic enhancers. These

eRNA read densities were averaged using a geometric mean within a genotype (n=2 retinas per condition) and changes were compared.

For eRNA aggregate plots, HOMER 4.1 was used. Reads that were on the transcribed sense strand within genes were removed from the analysis using a custom script. As described for ChIP-Seq, a tag directory was generated using MakeTagDirectory.pl with a fragment length of 90 and aggregate plots were generated using annotatepeaks.pl and options –d -size 6000 -hist 20.

To determine if the number of MEF2D ChIP-Seq peaks found near genes that are significantly misregulated in Mef2d KO retinas was enriched above random chance, Monte Carlo analysis was performed ($p<10^{-5}$; 10,000 iterations).

Reporter cloning

Luciferase reporters were generated by amplifying MEF2D-bound promoter or enhancer sequences from genomic DNA isolated from C57Bl6/J mouse tissue and cloning promoter regions into the pGL4.10 vector (Promega) using SacI and XhoI sites and enhancer regions into the pGL4.23 vector (Promega) using BamHI and SalI sites.

Primers used in cloning reporters

2610034M16Rik promoter

for: atgctagagctcAGCAAATATTAAAATAGACACC

rev: atgctactcgagTCATTTTGGCACAGGTTTC

Wdr17 promoter

for: atgctagagctcGCTACAAATGAAGTTATATGGC

rev: atgctactcgagGAATTGGTTTCTTGCTTTTC

Pcdh15 upstream enhancer

for: atgctaggatccTGTTGAATTTTAACTAAAG

rev: atgctagtcgacCAAACTGTTAAGAAATGTCA

Pcdh15 intronic enhancer

for: atgctaggatccTGCTTCTACGTTTTAAGCCA

rev: atgctagtcgacTTACCAGACATTTGCCTCAA

Fscn2 intronic enhancer

for: atgctaggatccAGTTTGTTGGAGGGAGCCCAA

rev: atgctagtcgacCAACAAGGAAGCTGCTCGCA

Guca1b upstream enhancer

for: atgctaggatccGGAGCACAGAACATACATGG

rev: atgctagtcgacTTCCTAGCCTGTGTGAGGGT

Pla2R1 intronic enhancer

for: atgctaggatccATTTCAGGCTTGTCTACAAT

rev: atgctagtcgacCTTTATCCTCACCAAGGCTA

Retinal explant luciferase reporter assays

The explant electroporation protocol was adapted from Matsuda and Cepko, 2008. Promoter or enhancer firefly luciferase reporters were co-electroporated into dissected retinas at p0 with a

control reporter constitutively expressing renilla luciferase. Retinas were cultured for 11 days and then washed briefly in ice cold 1x PBS and homogenized in 500µl passive lysis buffer with trituration. Homogenate was snap frozen to promote cell lysis and subsequently thawed for analysis of luciferase activity using the Dual-Glo® Luciferase Assay System (Promega). Firefly luciferase activity was normalized to renilla luciferase activity.

Supplemental References

Bailey, T.L., Boden, M., Buske, F.A., Frith, M., Grant, C.E., Clementi, L., Ren, J., Li, W.W., Noble, W.S. (2009) MEME SUITE: tools for motif discovery and searching. Nucleic Acids Res. *37*, W202-208.

Cherry, T.J., Wang, S., Bormuth, I., Schwab, M., Olson, J., Cepko, C.L. (2011) NeuroD factors regulate cell fate and neurite stratification in the developing retina. J Neurosci *31,* 7365-7379.

Dennis, G. Jr., Sherman, B.T., Hosack, D.A., Yang, J., Gao, W., Lane, H.C., Lempicki, R.A. (2003) DAVID: Database for Annotation, Visualization, and Integrated Discovery. Genome Biol *4*, P3.

Matsuda, T., Cepko, C.L. (2008) Analysis of gene function in the retina. Methods Mol Biol. *423*, 259-278.

Untergasser, A., Nijveen, H., Rao, X., Bisseling, T., Geurts, R., Leunissen, J.A. (2007) Nucleic Acids Res *35*, W71-74.